# The key role of inertia in the Plateau-Rayleigh instability for liquid-vapour water system

*GDR TransInter II*

23-25 septembre 2024


M. Rykner[1,2]

E. Saikali[1], A. Bruneton[1], B. Mathieu[3], V. Nikolayev [2,4]

[1]CEA - DES/ISAS/DM2S/SGLS/LCAN, [2]Université Paris-Saclay, [3]Université Grenoble Alpes, CEA Liten - DEHT/SAMA/LMPS, [4]CEA - DRF/IRAMIS/SPEC/SPHYNX

The **Plateau-Rayleigh instability** can be observed on wetted wires where, to **minimize its surface**, water organizes itself as regularly spaced **droplets**...

The **Plateau-Rayleigh instability** can be observed on wetted wires where, to **minimize its surface**, water organizes itself as regularly spaced **droplets**...

... but it is also observed on **capillaries**.

The **Plateau-Rayleigh instability** can be observed on wetted wires where, to **minimize its surface**, water organizes itself as regularly spaced **droplets**...

... but it is also observed on **capillaries**.

# Proton Exchange Membrane Fuel Cell (PEMFC)

Fuel cells convert **hydrogen** into **electricity**

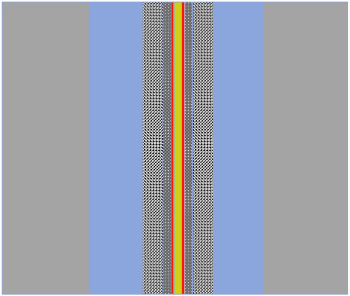

⚠Not to scale.

# Proton Exchange Membrane Fuel Cell (PEMFC)

## Fuel cells convert **hydrogen** into **electricity**

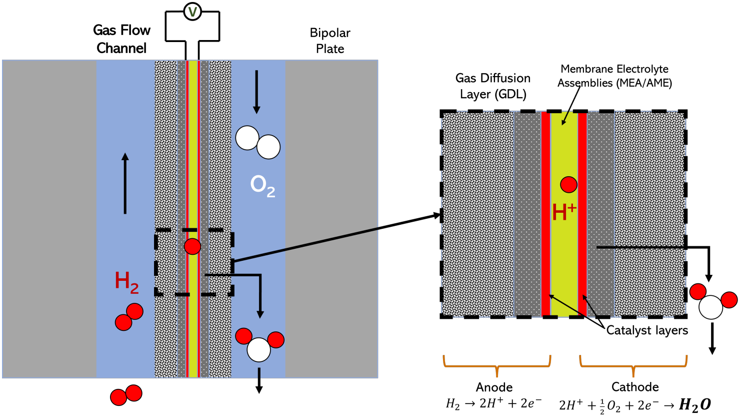


⚠Not to scale.

**How to evacuate water ?**

# Objectives

**Two-phase flow regimes: films and plugs**

**Film flow**

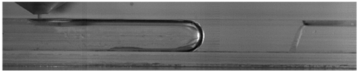

**Plug flow**

# Objectives

## Two-phase flow regimes: films and plugs

**Film flow**

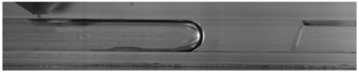

**Plug flow**

### Objectives

1. Is the lubrication approach enough to model the plug formation phenomenon ?
2. If not, what is the role played by inertia ?

**Tool: TRUST/TrioCFD - Front-Tracking / Analytical models**

# Lubrication model

Lubrication theory for a **water film** in presence of a **flow** $Q_0$
2D Axisymmetric model

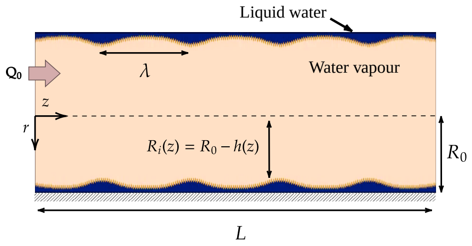


- Geometry: 0.5 mm-radius axisymmetric pipe.
- Incompressible and laminar flows.
- Gravity, interfacial phase change and thermal effects are neglected.

# Lubrication model

Lubrication theory for a **water film** in presence of a **flow** $Q_0$
2D Axisymmetric model

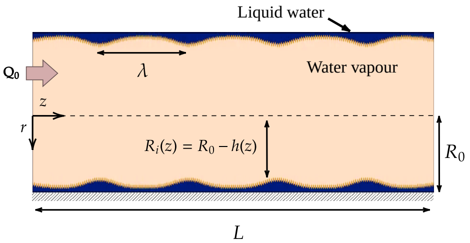


- Geometry: 0.5 mm-radius axisymmetric pipe.
- Incompressible and laminar flows.
- Gravity, interfacial phase change and thermal effects are neglected.

**Our lubrication model**

$$-2\pi R_i \frac{\partial h}{\partial t} = Q_0 \alpha \frac{\partial h}{\partial z} + \sigma \frac{\partial}{\partial z}\left[\beta\left(\frac{\partial^3 h}{\partial z^3} + \frac{\partial h}{\partial z}\frac{1}{R_i^2}\right)\right] \quad (1)$$

with $\alpha(h)$ and $\beta(h)$.

# DNS *vs* Lubrication

## Comparison between Front-Tracking and Lubrication theory:

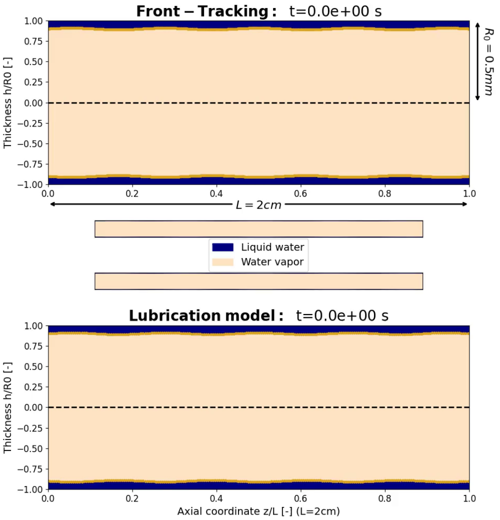


$$Q_0 = 0, \epsilon = h_0/R_0 = \mathbf{0.1}$$

# DNS *vs* Lubrication

## Comparison between Front-Tracking and Lubrication theory:

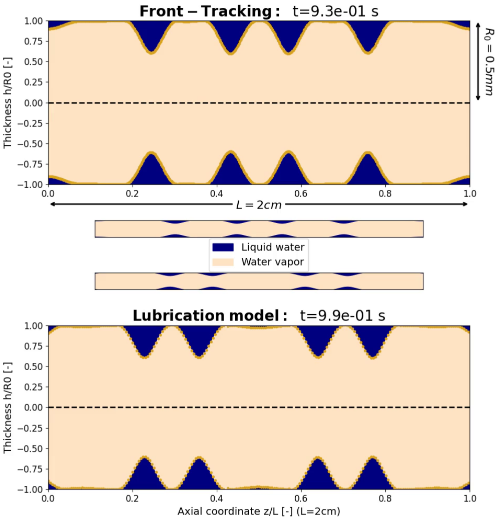


$$Q_0 = 0,\ \epsilon = h_0/R_0 = \mathbf{0.1}$$

- **Agreement** of Front-Tracking simulations with lubrication theory.
- **Stable collars are formed**, as expected by [Gauglitz and Radke, 1988].

# DNS *vs* Lubrication

## Comparison between Front-Tracking and Lubrication theory:

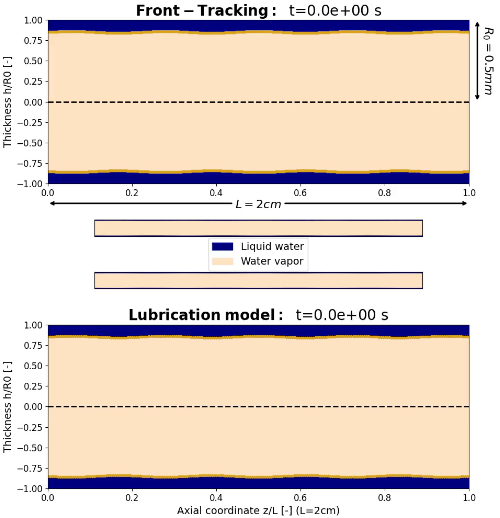


$$Q_0 = 0, \epsilon = h_0/R_0 = \mathbf{0.15}$$

# DNS *vs* Lubrication

## Comparison between Front-Tracking and Lubrication theory:

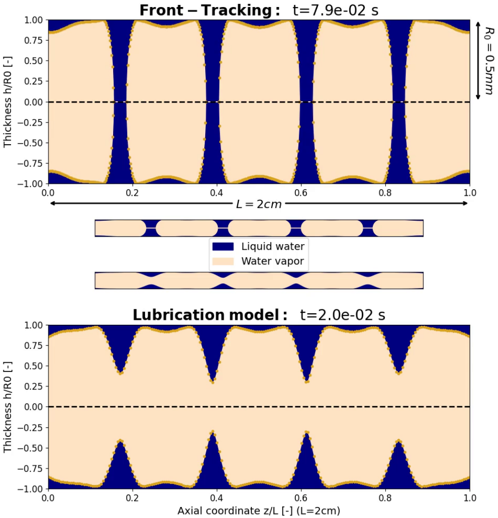


$$Q_0 = 0, \epsilon = h_0/R_0 = \mathbf{0.15}$$

- **Plugs are formed**, as predicted by [Gauglitz and Radke, 1988].
- Plug formation is **slower in Front-Tracking** simulations

  $\rightarrow$ **inertia**.
- Linear stability models **accounting for inertia** are developed.

# Linear stability analysis: effect of inertia

**Effect of wavenumber $x = kR_i$ on the instability growth rate $\hat{\omega} = \omega \frac{\mu_l R_i}{\sigma}$**

Lubrication & thin film : $\hat{\omega} = \frac{\epsilon^3}{3} x^2 \left(1 - x^2\right)$

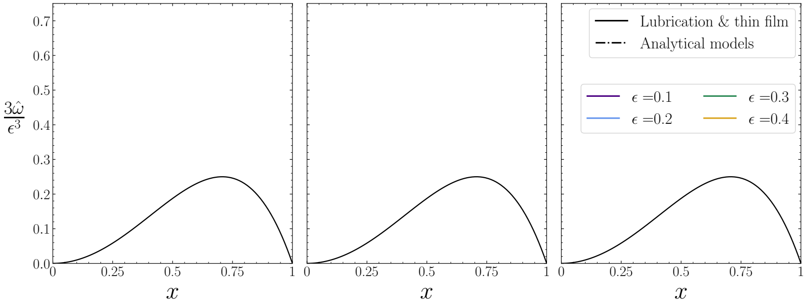

# Linear stability analysis: effect of inertia

**Effect of wavenumber $x = kR_i$ on the instability growth rate $\hat{\omega} = \omega \frac{\mu_l R_i}{\sigma}$**

Lubrication & thin film : $\hat{\omega} = \frac{\epsilon^3}{3} x^2 \left(1 - x^2\right)$

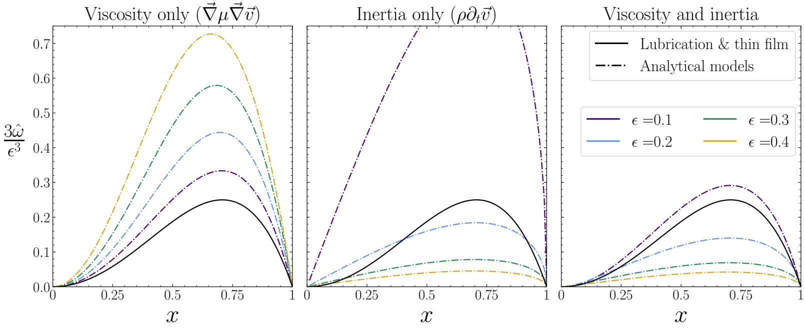

# Linear stability analysis: effect of inertia

**Effect of wavenumber $x = kR_i$ on the instability growth rate $\hat{\omega} = \omega \frac{\mu_l R_i}{\sigma}$**

Lubrication & thin film : $\hat{\omega} = \frac{\epsilon^3}{3} x^2 \left(1 - x^2\right)$

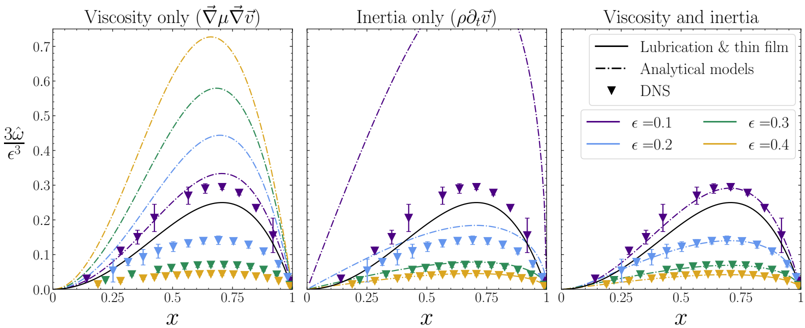


- The existence of a **viscous** ($\epsilon \leq 0.1$) and an **inertial** ($\epsilon \geq 0.2$) regimes is evidenced.
- DNS **perfectly agrees** with the complete model (inertia+viscosity).

# Linear stability analysis: effect of inertia

**Maximum growth rate as a function of $\epsilon$**

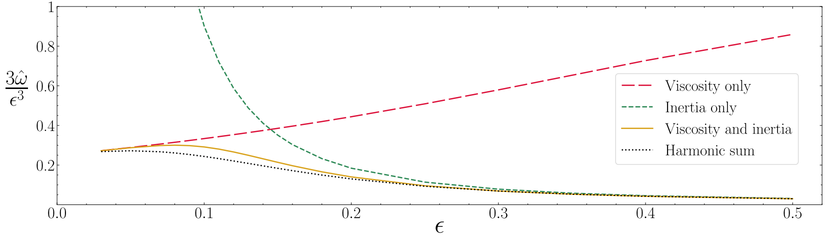


- The existence of a **viscous** ($\epsilon \leq$ 0.1) and an **inertial** ($\epsilon \geq$ 0.2) regimes is evidenced.
- Inertial and viscous effects are not perfectly independent.

# Effect of the core vapour

**Effect of the viscosity ratio $m = \frac{\mu_g}{\mu_l}$ without inertia**

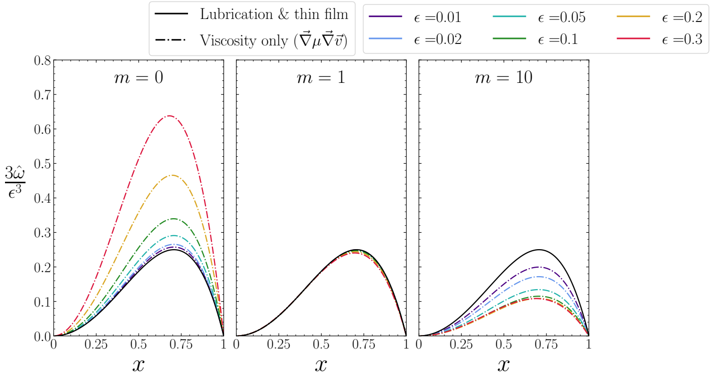


- The more viscous is the core fluid, the slower is the instability.
- Same for density: the denser the core fluid, the slower the instability.

# Effect of the core vapour

**Effect of the viscosity ratio $m = \frac{\mu_g}{\mu_l}$ without inertia**

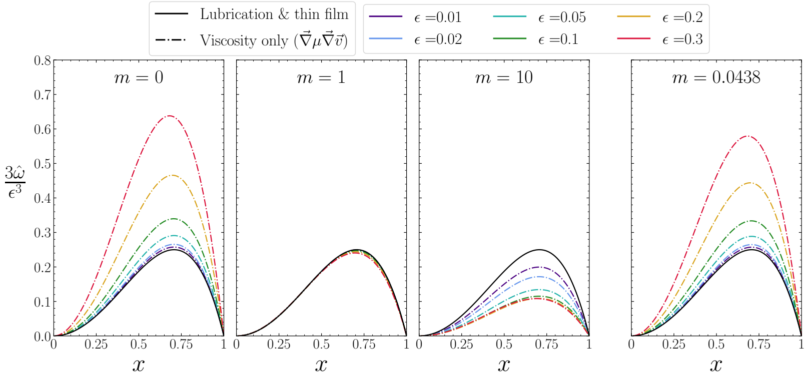


- The more viscous is the core fluid, the slower is the instability.
- Same for density: the denser the core fluid, the slower the instability.
- In the liquid/vapour water case, the vapour influence is negligible **without vapour flow**

# Contribution maps: linear regime

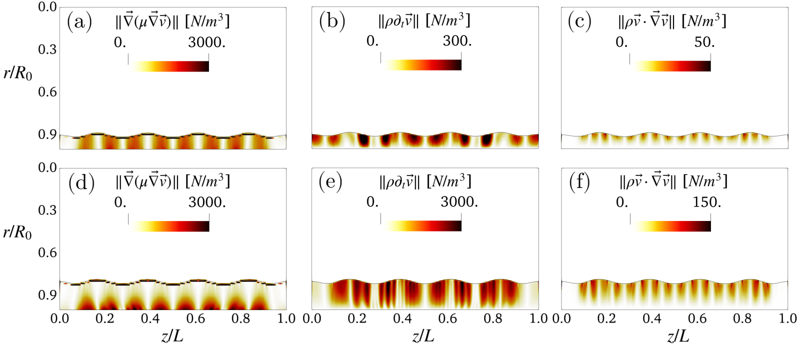


**a-c** : thin film ($\epsilon = 0.1$) - **d-f** : thick film ($\epsilon = 0.2$).

# Contribution maps: linear regime

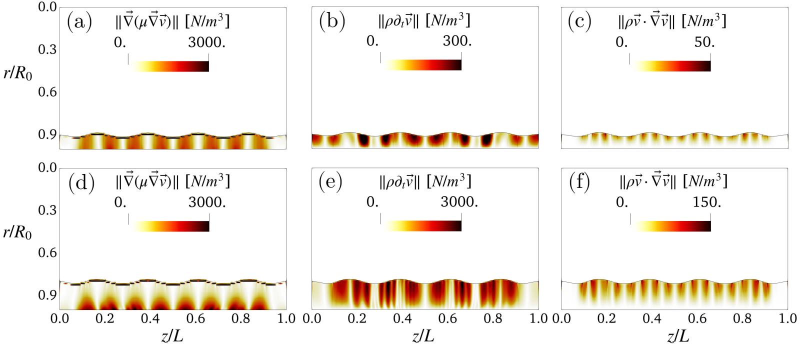


**a-c** : thin film ($\epsilon = 0.1$) - **d-f** : thick film ($\epsilon = 0.2$).

- Viscosity dominates the **thin** film regime.
- Viscosity and inertia are **spatially separated** in the **thick** film regime.
  $\rightarrow$ Change in the nature of the kinetic energy transport.

# Contribution maps: plug formation (1/2)

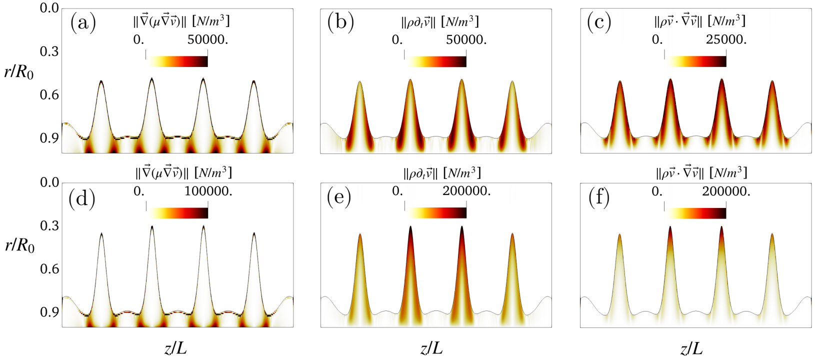


thick film ($\epsilon = 0.2$) - **a-c** : 18 ms - **d-f** : 19 ms - **g-h** : 20 ms.

# Contribution maps: plug formation (1/2)

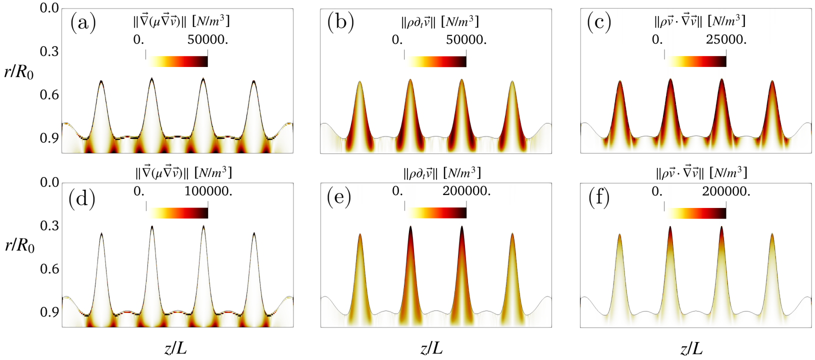


thick film ($\epsilon = 0.2$) - **a-c** : 18 ms - **d-f** : 19 ms - **g-h** : 20 ms.

- **Inertia and convection** dominates the behaviour right before occlusion.

# Contribution maps: plug formation (2/2)

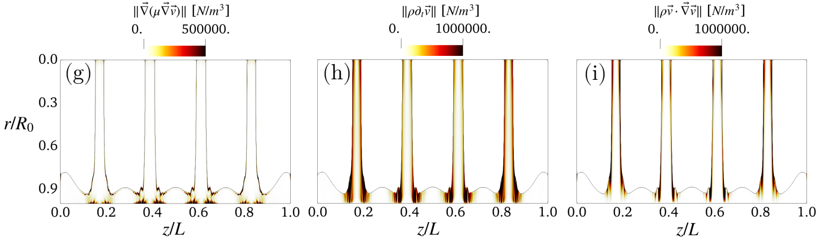


- Generation of **capillary waves** after occlusion.
  $\rightarrow$ dissipated by viscosity.

# Plug formation and capillary waves (1/2)

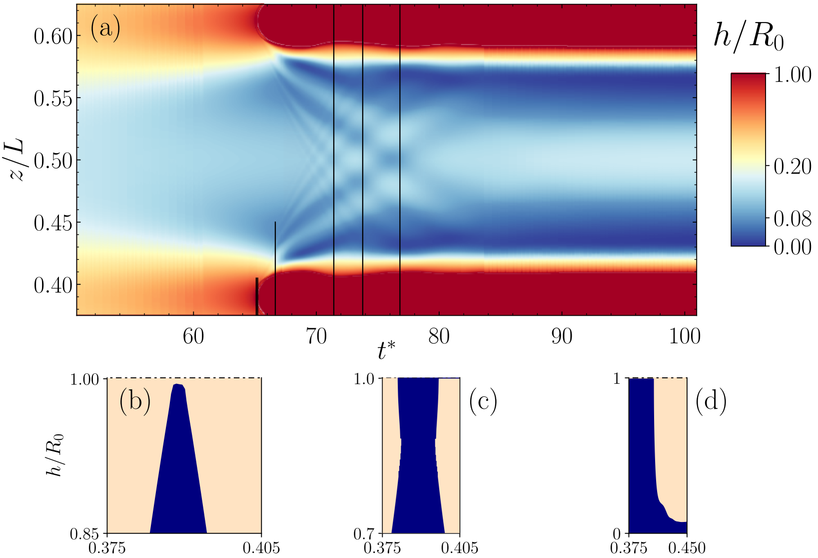

# Plug formation and capillary waves (2/2)

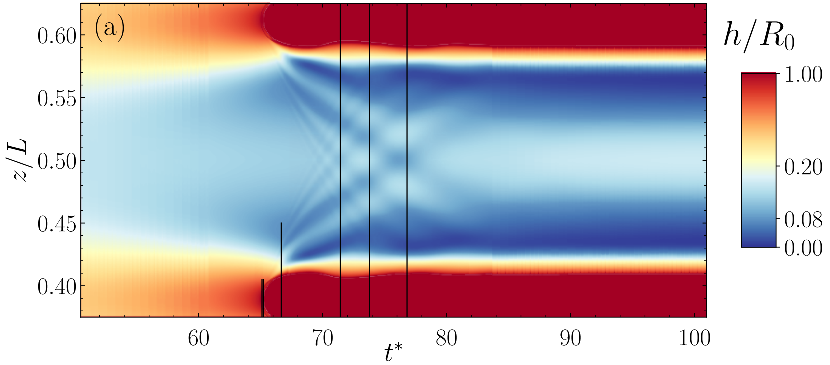


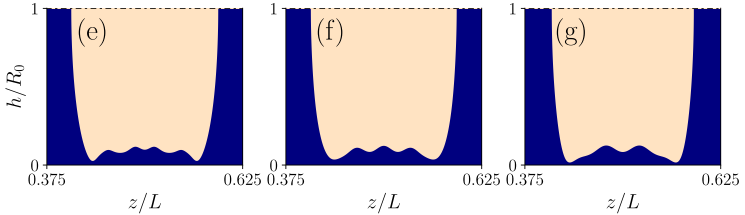

## Conclusion

- Existence of a **viscous** and an **inertial** regimes of the Plateau-Rayleigh instability.
- Inertia is **critical** to the plug formation in liquid/vapour water systems.
- What happens with an external flow $Q_0$ ?

## Conclusion

- Existence of a **viscous** and an **inertial** regimes of the Plateau-Rayleigh instability.
- Inertia is **critical** to the plug formation in liquid/vapour water systems.
- What happens with an external flow $Q_0$ ?

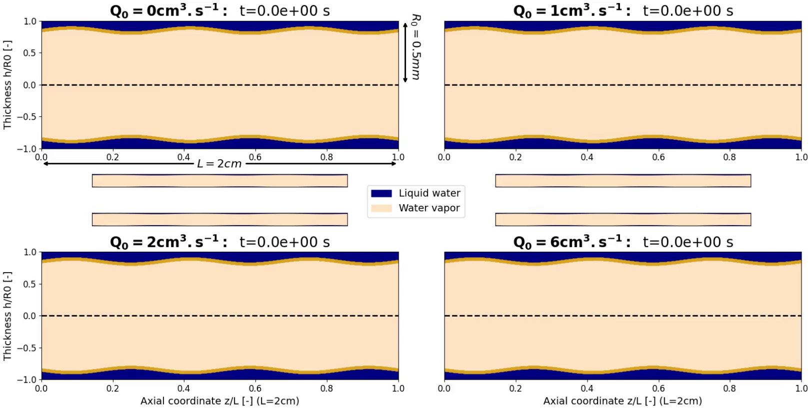

## Conclusion

- Existence of a **viscous** and an **inertial** regimes of the Plateau-Rayleigh instability.
- Inertia is **critical** to the plug formation in liquid/vapour water systems.
- What happens with an external flow $Q_0$ ?

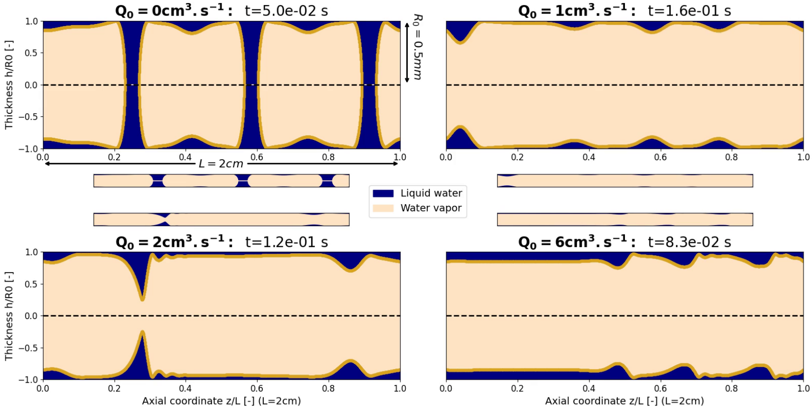

# Presence of air flow - permanent regime

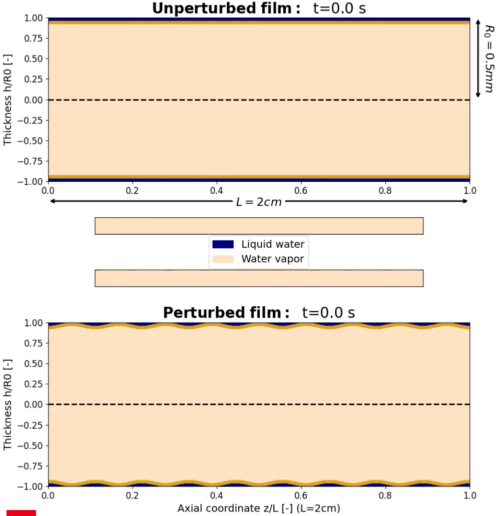


$$Q_g = 0.8\,\mathrm{cm}^3,$$
$$Q_l = 0.4\,\mathrm{mm}^3,$$
$$\epsilon = h_0/R_0 = 0.06$$

# Presence of air flow - permanent regime

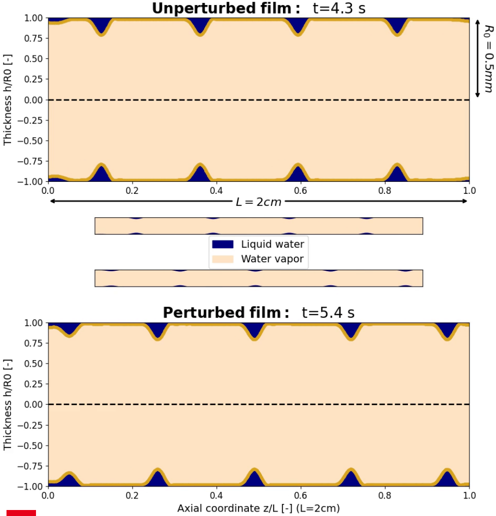


$$Q_g = 0.8\,\text{cm}^3,$$
$$Q_l = 0.4\,\text{mm}^3,$$
$$\epsilon = h_0/R_0 = 0.06$$

- Obtention of a **permanent regime**.
- Same flow rates and boundary conditions, but distinct initial conditions
  $\rightarrow$ **the same regime is observed**.

Thank you for your attention

# Appendix: DNS validation (1/3)

## Time and mesh convergence analysis

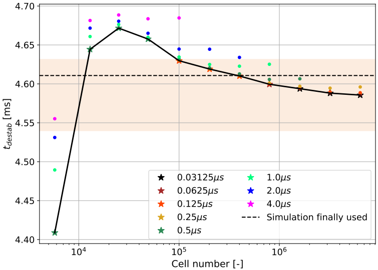


(a) $t_{destab}$

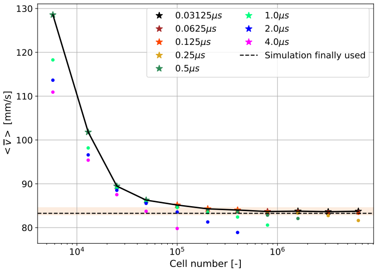


(b) $<\overline{v}>_{[0.9t_p;t_p]}$

Figure 1: Color of the point = timestep.
Stars and plain line = smaller timestep.
Dashed line = mesh and timestep finally used (locally refined).
Colored area = 1% gap to converged value.

# Appendix: DNS validation (2/3)

## Evolution of the maximal amplitude with respect to dimensionless time

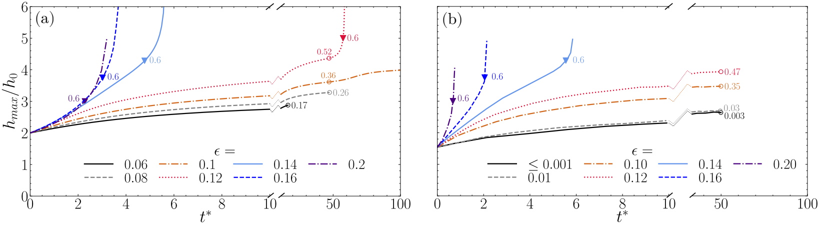


- Same evolution as [Gauglitz and Radke, 1988]. Same critical $\epsilon$ between collars and plugs.

# Appendix: DNS validation (3/3)

## Velocity fields around plug formation

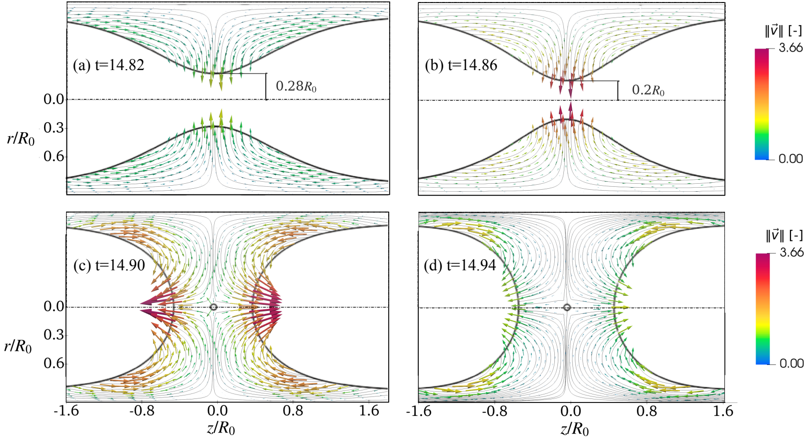


- Similar results as [Bian et al., 2010, Tai et al., 2011, Romanò et al., 2019].

# Appendix: Analytical models (1/4)

- Expression of velocities with a current function $\psi$ to respect mass conservation:

$$v_r = \frac{1}{r}\frac{\partial \psi}{\partial z} \quad \text{and} \quad v_z = -\frac{1}{r}\frac{\partial \psi}{\partial r}. \tag{2}$$

- Navier-Stokes equations transformed to:

$$\left(D - \frac{1}{\nu}\frac{\partial}{\partial t}\right) D\psi = 0, \tag{3}$$

with $D = \frac{\partial^2}{\partial r^2} - \frac{1}{r}\frac{\partial}{\partial r} + \frac{\partial^2}{\partial z^2}$.

- In the case with viscosity and inertia,

$$\psi_g = [C_g I_1(kr) + D_g I_1(k_g r)]\, r \exp(i\omega t + ikz),$$
$$\psi_l = [A_l K_1(kr) + B_l K_1(k_l r) + C_l I_1(kr) + D_l I_1(k_l r)]\, r \exp(i\omega t + ikz),$$

with $k_{l,g}^2 = k^2 + i\omega/\nu_{l,g}$

# Appendix: Analytical models (2/4)

- Six boundary conditions converted into six equations to give the six coefficients.
- Identical to finding $\hat{\omega}$ such that $\det \boldsymbol{M} = 0$ with

$$\boldsymbol{M} = \begin{bmatrix} 0 & 0 & K_1(ax) & K_1(ax_l) & I_1(ax) & I_1(ax_l) \\ 0 & 0 & -K_0(ax) & -\frac{x_l}{x}K_0(ax_l) & I_0(ax) & \frac{x_l}{x}I_0(ax_l) \\ I_1(x) & I_1(x_g) & -K_1(x) & -K_1(x_l) & -I_1(x) & -I_1(x_l) \\ I_0(x) & \frac{x_g}{x}I_0(x_g) & K_0(x) & \frac{x_l}{x}K_0(x_l) & -I_0(x) & -\frac{x_l}{x}I_0(x_l) \\ (m-1)I_1(x) & \left[(m-1) - \frac{\hat{\omega}J_g}{2x^2}\right] I_1(x_g) & 0 & \frac{\hat{\omega}J_l}{2x^2}K_1(x_l) & 0 & \frac{\hat{\omega}J_l}{2x^2}I_1(x_l) \\ F_1' & F_2' & \hat{\omega}J_l K_0(x) & 0 & -\hat{\omega}J_l I_0(x) & 0 \end{bmatrix}$$

with:

$$F_1' = 2(1-m)x^2 I_1'(x) + \hat{\omega}J_g I_0(x) + x\frac{x^2-1}{\hat{\omega}}I_1(x)$$

$$F_2' = 2(1-m)x_g x I_1'(x_g) + x\frac{x^2-1}{\hat{\omega}}I_1(x_g)$$

# Appendix: Analytical models (3/4)

- Similarly, if only viscosity is considered, one wants to find $\hat{\omega}$ such that $\det \boldsymbol{M} = 0$ with

$$\boldsymbol{M} = \begin{bmatrix} 0 & 0 & K_1(ax) & axK_0(ax) & I_1(ax) & axI_0(ax) \\ 0 & 0 & -K_0(ax) & f_k(ax) & I_0(ax) & f_i(ax) \\ I_1(x) & xI_0(x) & -K_1(x) & -xK_0(x) & -I_1(x) & -xI_0(x) \\ I_0(x) & f_i(x) & K_0(x) & -f_k(x) & -I_0(x) & -f_i(x) \\ (m-1)I_1(x) & mI_1(x)+(m-1)xI_0(x) & 0 & K_1(x) & 0 & -I_1(x) \\ G_1' & G_2' & K_1(x) & 0 & I_1(x) & 0 \end{bmatrix}$$

with:

$$f_k(x) = 2K_0(x) - xK_1(x),$$
$$f_i(x) = 2I_0(x) + xI_1(x),$$
$$G_1' = (1-m)xI_0(x) + (m-2)I_1(x) + \frac{x^2-1}{2\hat{\omega}} I_1(x),$$
$$G_2' = (1-m)x^2 I_1(x) + x\frac{x^2-1}{2\hat{\omega}} I_0(x).$$

# Appendix: Analytical models (4/4)

- If only inertia is considered:

$$\boldsymbol{M} = \begin{bmatrix} 0 & K_1(ax) & I_1(ax) \\ I_1(x) & -K_1(x) & -I_1(x) \\ F_1' & \hat{\omega} J_l K_0(x) & -\hat{\omega} J_l I_0(x) \end{bmatrix}$$

with $F_1' = x\dfrac{x^2-1}{\hat{\omega}} I_1(x) + \hat{\omega} J_g I_0(x)$

# Appendix: Contribution maps for collar formation

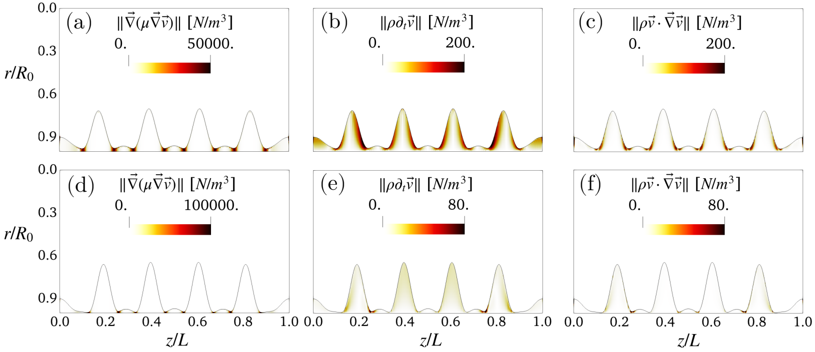


thin film ($\epsilon = 0.1$) - **a-c** : 100 ms - **d-f** : 300 ms

- Inertia plays no role neither on the formation nor on the motion of collars.
- A lubrication approach is enough to describe thin film evolution.

# Appendix: imposed air flow

## Permanent regime:

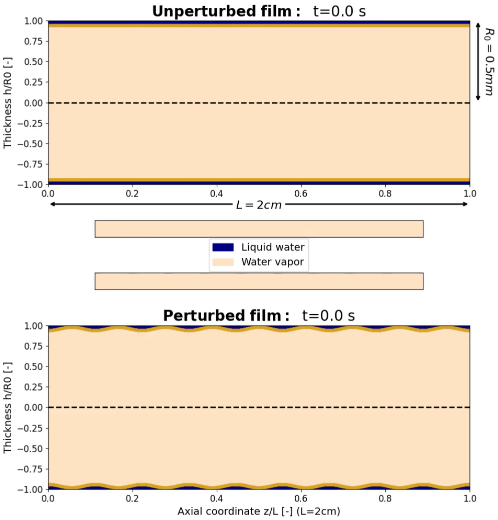


$$Q_g = 0.8\,\mathrm{cm}^3,$$
$$Q_l = 0.4\,\mathrm{mm}^3,$$
$$\epsilon = h_0/R_0 = 0.06$$

- Obtention of a **permanent regime**.
- Same flow rates and boundary conditions, but distinct initial conditions
  $\rightarrow$ **the same regime is observed**.